Smart Structures and Systems, *Vol. 19, No. 2 (2017) 213-224*
DOI: https:// doi.org/10.12989/sss.2017.19.2.213

Electromechanical coupled nonlinear dynamics of euler beam rails for electromagnetic railgun

Lizhong Xu* and Dewen Wu

Mechanical engineering institute, Yanshan University, Qinhuangdao, 066004, China

(Received April 17, 2016, Revised November 11, 2016, Accepted November 18, 2016)

Abstract. The electromagnetic field can cause an essential change of the dynamic behavior of the railgun. The evaluation of the dynamics performance of railgun is a mandatory task. Here, a nonlinear electromagnetic force equation of the railgun is given in which the clearance, the thickness and the width of the rail are considered. Based on it, the nonlinear electromechanical coupled dynamics equations of Euler beam rails for the railgun are proposed. Using the equations, the nonlinear free vibration frequency of the railgun is investigated and the effects of the system parameters on the frequency are analyzed. The nonlinear forced responses of the rail to the electromagnetic excitation are investigated as well. The results show that as the nonlinearity of the railgun system is considered, the vibration frequencies of the railgun system increase; as the current in the rail increases, the difference between the natural frequencies and the nonlinear vibration frequencies increases significantly; the nonlinearity of the railgun system is more obvious for smaller distance between the two rails, smaller rail thickness, and smaller stiffness of the elastic foundation; the unstable dynamics state of the rail system occurs when the armature runs to the exit of the railgun. The results are useful for design and application of the railgun system.

Keywords: railgun; nonlinear dynamics; vibration frequency; electromechanical coupled

1. Introduction

The railgun is an attractive electromagnetic gun due to its apparent simple design. The muzzle velocities up to 2.5 km/s for masses of several hundred grams have been demonstrated experimentally (Fair 2007, Shvetsov, Rutberg *et al.* 2007, Lehmann, Peter *et al*. 2001). The railgun includes two parallel copper rails across which an armature makes electrical contact (see Fig. 1). The rails are copper strips $h \times b$ and length L. The distance between the two rails is d. A large current I pass through the rails and the armature (projectile), and the projectile current interacts with the strong magnetic fields generated by the rails and the armature. It produces a strong force to accelerate the armature together with the projectile along the rails. Meanwhile, a mutually repulsive force occurs between the two rails.

The dynamics behavior of the railgun is of great importance for the system's performance. In the railgun, the mechanical response of the rail to the transient magnetic load may lead to disturbances of the projectile trajectory because the armature performance is very sensitive to variations of normal forces at the contact interface. Therefore, the evaluation of the dynamics performance of railgun is a mandatory task for the railgun system. For the dynamic behavior of the electromagnetic railguns, the first model is to take the rail as one-dimensional beam on an elastic foundation (Fryba 1977). The dynamic response of the railgun to the moving magnetic excitation was investigated (Tzeng 2003, Tzeng and Sun 2007). The axis-symmetric shell and two-dimensional solid models were used to simulate the railgun and numerically study the transient resonance at critical velocities of the projectile (Nechitailo and Lewis 2006). The transient elastic waves in electromagnetic launchers and their influence on armature contact pressure were studied (Johnson and Moon 2006, 2007). A 2D plane stress finite element model resting upon discrete elastic supports was developed and the transient analysis for a set of constant loading velocities was performed (Tumonis, Liudas *et al*. 2009). Equations for the forced responses of the rail to constant velocity load and the acceleration load were developed and the dynamic displacements of the rail under the running electromagnetic forces for various accelerations were studied (Xu and Geng 2012).

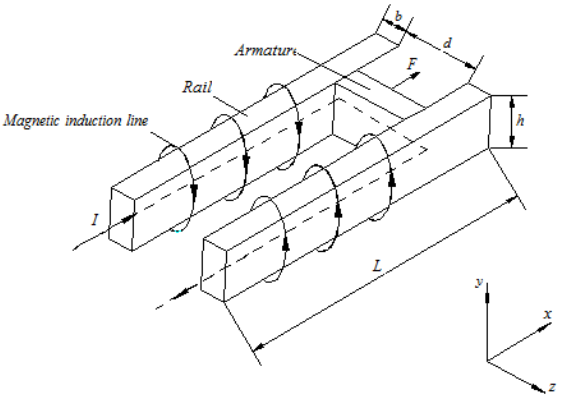

Fig. 1 Schematic of railgun

*Corresponding author, Professor
E-mail: xlz@ysu.edu.cn
[a] Master
E-mail: 296385330@qq.com

ISSN: 1738-1584 (Print), 1738-1991 (Online)

For the railgun, a generalized dynamic stiffness method for analysis was proposed and three characteristic speeds (critical, shear, and bar speeds) were analyzed. Here, Timoshenko beam model is used and bending deformation plus shearing deformation can be considered. Using the model, the influences of cross-sectional warpings on these characteristic speeds were investigated (Pai, Frank *et al*. 2012). The vibration experiment of a railgun with discrete supports was done (Schuppler, Christian *et al*. 2013). The rails of rectangular electromagnetic rail gun were simplified as a double layer elastic foundation beam, and the dynamic response of the rails was investigated (He and Bai 2013).

In railgun, the electromagnetic field can cause an essential change of the dynamics behaviors of the railgun. The linear electromechanical coupled effects were considered, and the natural frequencies of the railgun were investigated (Geng 2013). In operation, the rail current is quite large which causes the strong electromagnetic nonlinearity in the railgun system. So, the electromechanical coupled nonlinear free vibration of the railgun system was studied (Xu, Zheng *et al*. 2015). However, there are two shortcomings in above analysis: (1). the nonlinear electromagnetic force is only expressed as a function of the distance between the two rails. It ignores some main parameters. The effects of these parameters on the electromechanical coupled nonlinear free vibration of the railgun system can not be considered. (2). the rail current is taken as the nonlinear parameter which is not convenient because the rail current is variable during the railgun operation. Besides it, the electromechanical nonlinear coupled response of the railgun to the electromagnetic excitation has not been investigated yet.

In this paper, the nonlinear electromechanical coupled dynamics equations for the railgun were deduced. Using the equations, the nonlinear free vibration frequency of the railgun and the nonlinear forced responses of the railgun to the electromagnetic excitation were investigated. Compared to other research work, the effects of the distance between two rails, the thickness and the width of the rail on the nonlinear dynamics performance of the railgun were considered. Here, the ratio of the rail thickness to the distance between the two rails is taken as the nonlinear parameter which is convenient to study the nonlinear forced responses of the railgun to the electromagnetic excitation. We obtain some novel results as below:

(1) As the nonlinearity of the railgun system is considered, the vibration frequencies of the railgun system increase. As the current in the rail grows, the difference between the natural frequencies and the nonlinear vibration frequencies grows significantly.

(2) The railgun system is a natural frequency changing system caused by the nonlinear electromagnetic force and the armature moving on the rail. For large armature position, the nonlinearity of the railgun system is more significant.

(3) The nonlinearity of the railgun system is more obvious for small distance between the two rails, small rail thickness, and small stiffness of the elastic foundation.

(4) As the rail current or the rail position coordinate grows, the unstable frequency range increases obviously. As the distance between two rails, the rail thickness, the rail width or the stiffness of the elastic foundation drop, the unstable frequency range increases obviously as well.

(5) When the armature runs to the exit, the vibrating amplitude of the forced responses of the rail to the electromagnetic load is the largest.

The results can be used to design dynamics performance of the railgun system.

2. Nonlinear electromagnetic force on the rail

When the current flows in the rails, a magnetic flux is produced between the rails and in the armature. It interacts with the current flowing in the projectile to cause Lorentz force which accelerates the armature and the projectile. Meanwhile, a nonlinear magnetic force occurs between the two rails. The nonlinear magnetic force per unit length between the two rails is (Geng (2013), here, only electromagnetic force between the two rails is considered. The current densities in the two rails are considered to be uniform)

$$q_{r0} = K_r I^2 \tag{1}$$

$$K_r = \frac{\mu_0}{4\pi h^2 b^2}\int_d^{d+b}\int_{-h/2}^{h/2}\int_{-b}^{0}\int_{-h/2}^{h/2}\frac{(z-z')}{\left[(y-y')^2+(z-z')^2\right]}\left[\frac{x}{\sqrt{(y-y')^2+(z-z')^2+x^2}}-\frac{x-l}{\sqrt{(y-y')^2+(z-z')^2+(x-l)^2}}\right]dy'dz'dydz \tag{2}$$

where μ_0 is the permeability, I is the current intensity in the rail, l is the running position of the armature, x is the position coordinate in the direction of the rail length, b is the thickness of the rail, h is the width of the rail, d is the distance between the two rails, $P'(z',y')$ is one point on the left rail, $P(z,y)$ is one point on the right rail.

Using Eqs. (1) and (2), we can calculate electromagnetic force applied to the rail. Results show:

When x=[l, L], the electromagnetic force is zero. When x=[0, l], the electromagnetic force is distributed uniformly on this part of the rail. Only near to x=0 or x=l, the electromagnetic force reduce to zero rapidly. The local force decrease has little effects on the rail elastic displacement. It mainly depends on almost uniform electromagnetic force. For simplifying calculation, we can considered that the distribution of the electromagnetic force on the rail is

$$\begin{cases} q_r = q_{r0} & (0 < x \le l) \\ q_r = 0 & (l < x < L) \end{cases}$$

Under this assumption, by means of the regressive interpolation, the nonlinear electromagnetic force as a function of the distance d , the width h, and the thickness b can be given as below

$$K_r = \frac{1.2101\times10^{-3}\left(0.01244h^3 - 0.001221h^2 - 4.296\times10^{-6}h + 6.809\times10^{-6}\right)}{(d+0.01343)(b+0.02622)} \tag{3}$$

The calculative results by Eq. (3) are compared with ones by Eq. (1) (see Fig. 2). It shows that the two results are in agreement with each other.

Considering the elastic displacement of the rail, the nonlinear magnetic force per unit length on the rail can be calculated as

$$\begin{cases} q_r = q_{r0} = \dfrac{1.2101\times10^{-3}\left(0.01244h^3 - 0.001221h^2 - 4.296\times10^{-6}h + 6.809\times10^{-6}\right)}{(d+2w_0+0.01343)(b+0.02622)} I^2 & (0<x<l) \\ q_r = 0 & (l<x<L) \end{cases} \quad (4)$$

where w_0 is the average static elastic displacement of the rail.

The magnetic force can be expressed in Fourier series form as

$$q_r = q_{r0}\left[\frac{l}{L} + \sum_1^{\infty}\frac{2}{n\pi}\sin\frac{n\pi l}{L}\cos\frac{n\pi x}{L}\right] \quad (5)$$

Substituting Eq. (5) into the force balance equation of the rail, yields

$$EI_z\frac{\partial^4 w}{\partial x^4} + kw = q_{r0}\left[\frac{l}{L} + \sum_1^{\infty}\frac{2}{n\pi}\sin\frac{n\pi l}{L}\cos\frac{n\pi x}{L}\right] \quad (6)$$

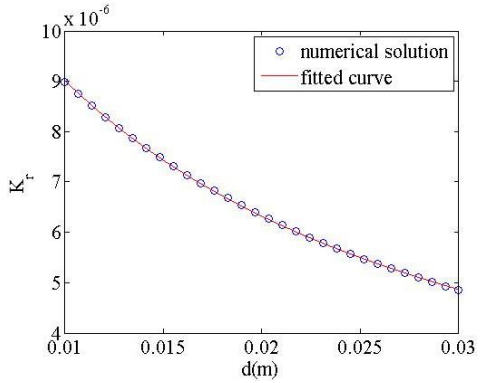

(a) *d* changes

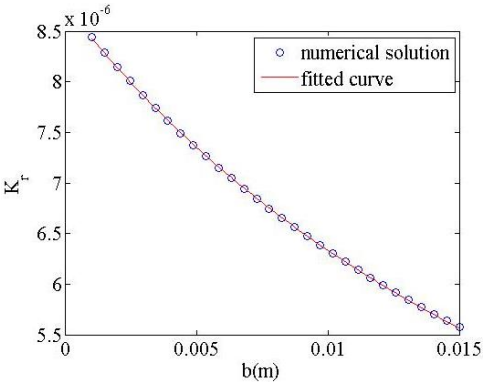

(b) *b* changes

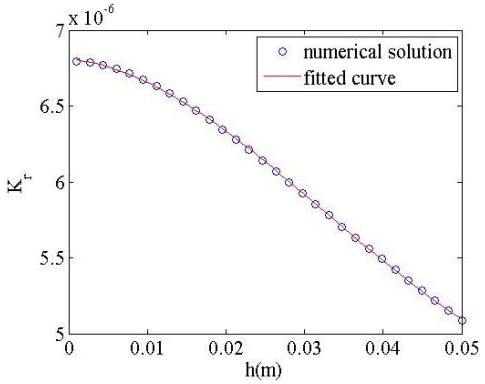

(c) *h* changes

Fig. 2 Comparison between the results by Eq.(1) and Eq.(3)

where E is the modulus of elasticity of the rail material, I_z is the sectional modular of the rail, k is the stiffness of the elastic foundation.

From Eq. (6), the elastic displacement w of the rail can be obtained

$$w = \frac{q_{r0}l}{Lk} + \sum_1^{\infty}\frac{2q_{r0}L^4}{EI_z n^5\pi^5 + nL^4k\pi}\sin\frac{n\pi l}{L}\cos\frac{n\pi x}{L} \quad (7)$$

The average displacement w_0 of the rail can be calculated as

$$w_0 = \frac{1}{l}\int_0^l w dx = \frac{q_{r0}l}{Lk} + \sum_1^{\infty}\frac{2q_{r0}L^5}{EI_z ln^6\pi^6 + n^2lL^4k\pi^2}\sin^2\frac{n\pi l}{L} \quad (8)$$

Combining Eq. (4) with (8), yields

$$\begin{aligned} &2w_0^2 + (d+0.01343)w_0 - \frac{1.2101\times10^{-3}\cdot\left(0.01244h^3 - 0.001221h^2 - 4.296\times10^{-6}h + 6.809\times10^{-6}\right)}{(b+0.02622)} \\ &\times I^2\left(\frac{l}{Lk} + \sum_1^{\infty}\frac{2L^5}{EI_z l\pi^6 n^6 + n^2lL^4k\pi^2}\sin^2\frac{n\pi l}{L}\right) = 0 \end{aligned} \quad (9)$$

Eq. (9) can give the average displacement w_0 of the rail. Results show that the average displacement w_0 of the rail is much smaller than clearance d. At a range of calculated parameters in this paper, it is smaller than 0.2 mm.

3. Electromechanical coupled nonlinear dynamics equations of the rail

The dynamic equation of the rail can be given as

$$\rho_l\frac{\partial^2\Delta w}{\partial t^2} + EI_z\frac{\partial^4\Delta w}{\partial x^4} + k\Delta w = \Delta q_r \quad (10)$$

where Δw is the dynamic displacement of the rail, ρ_l is the mass coefficient per unit length of the rail, Δq_r is the dynamic electromagnetic force on the rail.

The dynamic electromagnetic force can be expressed in series form as

$$\Delta q_r = \left.\frac{dq_r}{dw}\right|_{w_0}(w-w_0) + \frac{1}{2!}\left.\frac{d^2q_r}{dw^2}\right|_{w_0}(w-w_0)^2 + \cdots + \frac{1}{n!}\left.\frac{d^nq_r}{dw^n}\right|_{w_0}(w-w_0)^n \quad (11)$$

Combining Eq. (4) with (11), yields

$$\begin{cases} \Delta q_r = -\dfrac{2.4202\times10^{-3}\cdot K_{q3}\cdot I^2}{(d+2w_0+0.01343)^2(b+0.02622)}\Delta w + \dfrac{4.8404\times10^{-3}\cdot K_{q3}\cdot I^2}{(d+2w_0+0.01343)^3(b+0.02622)}\Delta w^2 + \ldots \\ \Delta q_r = 0 \qquad (l<x<L \end{cases} \quad (12)$$

$$0<x<L$$

where

$$K_{q3} = 0.01244h^3 - 0.001221h^2 - 4.296\times10^{-6}h + 6.809\times10^{-6}$$

Substituting Eq. (12) into (10), and letting the nonlinear parameter $\varepsilon = b/d$ for the railgun whose *b/d* is smaller than 1, yields

$$\begin{cases} \rho_l \dfrac{\partial^2 \Delta w}{\partial t^2} + EI_z \dfrac{\partial^4 \Delta w}{\partial x^4} + k\Delta w = -\dfrac{2.4202\times10^{-3}\cdot K_{q3}\cdot I^2}{\left(d+2w_0+0.01343\right)^2\left(b+0.02622\right)}\Delta w + \\ \dfrac{4.8404\times10^{-3}\cdot K_{q3}\cdot I^2\cdot d}{b\left(d+2w_0+0.01343\right)^3\left(b+0.02622\right)}\varepsilon\Delta w^2 - \\ \dfrac{4.8404\times10^{-3}\cdot K_{q3}\cdot I^2\cdot d}{b\left(d+2w_0+0.01343\right)^4\left(b+0.02622\right)}\varepsilon\Delta w^3+\cdots \qquad (0<x<l) \\ \rho_l \dfrac{\partial^2 \Delta w}{\partial t^2} + EI_z \dfrac{\partial^4 \Delta w}{\partial x^4} + k\Delta w = 0 \qquad (l<x<L) \end{cases} \tag{13}$$

Let $\Delta w = \phi(x)q(t)$, substituting it into the first equation of Eq. (13), yields

$$\frac{\ddot{q}(t)}{q(t)} - \varepsilon Q q(t) - \varepsilon Q_1 q(t)^2 = -\frac{EI\varphi^{(4)}(x) + P\varphi(x)}{\rho_l \varphi(x)} \quad (0<x<l) \tag{14}$$

where

$$P = k + \frac{2.4202\times10^{-3}\cdot K_{q3}\cdot I^2}{\left(d+2w_0+0.01343\right)^2\left(b+0.02622\right)}$$

$$Q = \frac{4.8404\times10^{-3}\cdot K_{q3}\cdot I^2\cdot d}{\rho_l b\left(d+2w_0+0.01343\right)^3\left(b+0.02622\right)}\overline{\varphi}$$

$$Q_1 = -\frac{4.8404\times10^{-3}\cdot K_{q3}\cdot I^2\cdot d}{\rho_l b\left(d+2w_0+0.01343\right)^3\left(b+0.02622\right)}\overline{\varphi}^2 \quad \left(\overline{\varphi} = \frac{1}{L}\int_0^L \varphi(x)dx\right)$$

Let Eq. (14) equal constant $-\omega^2$, thus

$$\ddot{q}(t) + \omega^2 q(t) - \varepsilon Q q^2(t) - \varepsilon Q_1 q^3(t) = 0 \tag{15}$$

$$\phi^{(4)}(x) - R\phi(x) = 0 \tag{16}$$

where $R = \dfrac{\omega^2\rho_l - P}{EI_z}$

Substituting $\Delta w = \phi(x)q(t)$ into the second equation of Eq. (13), yields

$$\phi^{(4)}(x) - S^4\phi(x) = 0 \tag{17}$$

where $S^4 = \dfrac{\omega^2\rho_l - k}{EI_z}$

From Eqs. (16) and (17) plus the boundary conditions and the continuity conditions of the rail, the natural frequencies and the mode functions of the rail can be obtained.

4. Electromechanical coupled nonlinear free vibration

Let

$$q(\tau,\varepsilon) = q_0 + \varepsilon q_1 + \varepsilon^2 q_2 + ... \tag{18}$$

and

$$\omega_n^2 = \omega^2(1 + \varepsilon\sigma_1 + \varepsilon^2\sigma_2 + \cdots) \tag{19}$$

where ω_n is the nonlinear vibration frequency of the rail considering electromechanical coupled effects.

Letting $\tau = \omega_n t$, and Eq. (15) can be changed into following form

$$\omega_n^2\ddot{q}(\tau) + \omega^2 q(\tau) - \varepsilon Q q^2(\tau) - \varepsilon Q_1 q^3(\tau) = 0 \tag{20}$$

Substituting Eqs. (18) and (19) into (20), and then let sum of the coefficients with the same order power equal zero, following equations can be given

$$\ddot{q}_0 + q_0 = 0 \tag{21a}$$

$$\ddot{q}_1 + q_1 = \frac{Q{q_0}^2 + Q_1{q_0}^3}{\omega^2} - \sigma_1\ddot{q}_0 \tag{21b}$$

$$\ddot{q}_2 + q_2 = \frac{2Qq_0q_1 + 3Q_1q_1{q_0}^2}{\omega^2} - \sigma_1\ddot{q}_1 - \sigma_2\ddot{q}_0 \tag{21c}$$

……

Here, initial conditions are

$$\left.\begin{array}{c} q_0(0) = Q_0, \dot{q}_0(0) = 0 \\ q_1(0) = 0, \dot{q}_1(0) = 0 \\ q_2(0) = 0, \dot{q}_2(0) = 0 \\ \cdots\cdots \end{array}\right\}$$

Then, solution of zero order equation under above initial conditions is

$$q_0 = Q_0\cos\tau \tag{22}$$

Substituting Eq. (22) into (21(b)), yields

$$\ddot{q}_1 + q_1 = \frac{QQ_0^2}{2\omega^2}\cos 2\tau + \frac{Q_0^2Q}{2\omega^2} + \frac{Q_1{Q_0}^3}{4\omega^2}\cos 3\tau + \left(\frac{3Q_1{Q_0}^3}{4\omega^2} + \sigma_1Q_0\right)\cos\tau \tag{23}$$

In order to remove secular item, let $\sigma_1 = -\dfrac{3Q_1{Q_0}^2}{4\omega^2}$, then

$$q_1 = \left(\frac{Q_1{Q_0}^3}{32\omega^2} - \frac{QQ_0^2}{3\omega^2}\right)\cos\tau - \frac{QQ_0^2}{6\omega^2}\cos 2\tau - \frac{Q_1{Q_0}^3}{32\omega^2}\cos 3\tau + \frac{QQ_0^2}{2\omega^2} \tag{24}$$

Substituting Eqs. (22) and (24) into (21(c)), yields

$$\begin{aligned} \ddot{q}_2 + q_2 = {} & -\frac{3Q_1^2Q_0^5}{128\omega^4}\cos 5\tau - \frac{5QQ_1Q_0^4}{32\omega^4}\cos 4\tau + \left(-\frac{Q^2Q_0^3}{6\omega^4} + \frac{3Q_1^2Q_0^5}{16\omega^4} - \frac{QQ_1Q_0^4}{4\omega^4}\right)\cos 3\tau + \\ & \left(-\frac{Q^2Q_0^3}{3\omega^4} + \frac{QQ_1Q_0^4}{\omega^4}\right)\cos 2\tau - \frac{Q^2Q_0^3}{3\omega^4} + \frac{21QQ_1Q_0^4}{32\omega^4} + \\ & \left[\frac{5Q^2Q_0^3}{6\omega^4} + \frac{3Q_1^2Q_0^5}{128\omega^4} - \frac{QQ_1Q_0^4}{2\omega^4} + \sigma_2Q_0\right]\cos\tau \end{aligned} \tag{25}$$

In order to remove secular item, let $\sigma_2 = \dfrac{QQ_1{Q_0}^3}{2\omega^4} - \dfrac{5Q^2Q_0^2}{6\omega^4} - \dfrac{3Q_1{}^2Q_0^4}{128\omega^4}$, then

$$\begin{aligned} q_2 = {} & \left(\frac{29Q^2Q_0^3}{144\omega^4} + \frac{23Q_1^2Q_0^5}{1024\omega^4} - \frac{35QQ_1Q_0^4}{96\omega^4}\right)\cos\tau - \frac{1}{3}\left(-\frac{Q^2Q_0^3}{3\omega^4} + \frac{QQ_1Q_0^4}{\omega^4}\right)\cos 2\tau - \\ & \frac{1}{8}\left(-\frac{Q^2Q_0^3}{6\omega^4} + \frac{3Q_1^2Q_0^5}{16\omega^4} - \frac{QQ_1Q_0^4}{4\omega^4}\right)\cos 3\tau + \frac{QQ_1Q_0^4}{96\omega^4}\cos 4\tau + \\ & \frac{Q_1^2Q_0^5}{1024\omega^4}\cos 5\tau - \frac{Q^2Q_0^3}{3\omega^4} + \frac{21QQ_1Q_0^4}{32\omega^4} \end{aligned} \tag{26}$$

Hence, solution of the nonlinear free vibration is

$$q(t)=Q_0\cos\omega_n t+\varepsilon\left[\left(\frac{Q_1Q_0^3}{32\omega^2}-\frac{QQ_0^2}{3\omega^2}\right)\cos\omega_n t-\frac{QQ_0^2}{6\omega^2}\cos 2\omega_n t-\frac{Q_1Q_0^3}{32\omega^2}\cos 3\omega_n t+\frac{QQ_0^2}{2\omega^2}\right]+$$
$$\varepsilon^2[(\frac{29Q^2Q_0^3}{144\omega^4}+\frac{23Q_1^2Q_0^5}{1024\omega^4}-\frac{35QQ_1Q_0^4}{96\omega^4})\cos\omega_n t-\frac{1}{3}\left(-\frac{Q^2Q_0^3}{3\omega^4}+\frac{QQ_1Q_0^4}{\omega^4}\right)\cos 2\omega_n t-$$
$$\frac{1}{8}(-\frac{Q^2Q_0^3}{6\omega^4}+\frac{3Q_1^2Q_0^5}{16\omega^4}-\frac{QQ_1Q_0^4}{4\omega^4})\cos 3\omega_n t+\frac{QQ_1Q_0^4}{96\omega^4}\cos 4\omega_n t+$$
$$\frac{Q_1^2Q_0^5}{1024\omega^4}\cos 5\omega_n t-\frac{Q^2Q_0^3}{3\omega^4}+\frac{21QQ_1Q_0^4}{32\omega^4}] \quad (27)$$

Equation of the magnitude and frequency relationship is

$$\omega_n^2=\omega^2[1-\frac{3Q_1{Q_0}^2}{4\omega^2}\varepsilon+(\frac{QQ_1{Q_0}^3}{2\omega^4}-\frac{5Q^2Q_0^2}{6\omega^4}-\frac{3{Q_1}^2{Q_0}^4}{128\omega^4})\varepsilon^2] \quad (28)$$

5. Electromechanical coupled forced responses

When the current excitation $\Delta I=I_m\cos(\omega_e t+\theta)$ (here, I_{m} is the magnitude of the excitation current, ω_e is its frequency), the electromagnetic force applied to the rail will fluctuate. The dynamic electromagnetic force can be expressed as

$$\Delta q=\left.\frac{\partial q}{\partial w}\right|_{(w_0,I)}\Delta w+\left.\frac{\partial q}{\partial I}\right|_{(w_0,I)}\Delta I+\left.\frac{1}{2!}\frac{\partial^2 q}{\partial w^2}\right|_{(w_0,I)}(\Delta w)^2+\left.\frac{1}{3!}\frac{\partial^3 q}{\partial w^3}\right|_{(w_0,I)}(\Delta w)^3+\cdots \quad (29)$$

Where

$$\left.\frac{\partial q}{\partial w}\right|_{(w_0,I)}=-\frac{2.4202\times10^{-3}\cdot K_{q3}\cdot I^2}{\left(d+2w_0+0.01343\right)^2\left(b+0.02622\right)}$$
$$\left.\frac{\partial q}{\partial I}\right|_{(w_0,I)}=\frac{2.4202\times10^{-3}\cdot K_{q3}\cdot I}{\left(d+2w_0+0.01343\right)\left(b+0.02622\right)}$$
$$\left.\frac{1}{2!}\frac{\partial^2 q}{\partial w^2}\right|_{(w_0,I)}=\frac{4.8404\times10^{-3}\cdot K_{q3}\cdot I^2}{\left(d+2w_0+0.01343\right)^3\left(b+0.02622\right)}$$
$$\left.\frac{1}{3!}\frac{\partial^2 q}{\partial w^2}\right|_{(w_0,I)}=-\frac{4.8404\times10^{-3}\cdot K_{q3}\cdot I^2}{\left(d+2w_0+0.01343\right)^4\left(b+0.02622\right)}$$

Letting the nonlinear parameter $\varepsilon=b/d$, and substituting Eq. (29) into (10) (considering damping term, here η is the damping factor), yields

$$\begin{cases}\rho_l\dfrac{\partial^2\Delta w}{\partial t^2}+EI_z\dfrac{\partial^4\Delta w}{\partial x^4}+\eta\dfrac{\partial\Delta w}{\partial t}+k\Delta w=-\dfrac{2.4202\times10^{-3}\cdot K_{q3}\cdot I^2}{\left(d+2w_0+0.01343\right)^2\left(b+0.02622\right)}\Delta w+\\ \dfrac{4.8404\times10^{-3}\cdot K_{q3}\cdot I_0^2\cdot d}{b\left(d+2w_0+0.01343\right)^3\left(b+0.02622\right)}\varepsilon\Delta w^2-\dfrac{4.8404\times10^{-3}\cdot K_{q3}\cdot I^2\cdot d}{b\left(d+2w_0+0.01343\right)^4\left(b+0.02622\right)}\varepsilon\Delta w^3\\ \qquad+\dfrac{2.4202\times10^{-3}\cdot K_{q3}\cdot I}{\left(d+2w_0+0.01343\right)\left(b+0.02622\right)}\Delta I \quad (0<x<l)\\ \rho_l\dfrac{\partial^2\Delta w}{\partial t^2}+EI_z\dfrac{\partial^4\Delta w}{\partial x^4}+\eta\dfrac{\partial\Delta w}{\partial t}+k\Delta w=0 \quad (l<x<L)\end{cases} \quad (30)$$

Substituting $\Delta w=\phi(x)q(t)$ into the first equation of Eq.(30), yields

$$\frac{\ddot q(t)}{q(t)}+\frac{\eta}{\rho_l}\frac{\dot q(t)}{q(t)}-\varepsilon Qq(t)-\varepsilon Q_1q(t)^2-\frac{2.4202\times10^{-3}\cdot K_{q3}\cdot I\cdot\Delta I}{\rho_l\bar\varphi\left(d+2w_0+0.01343\right)\left(b+0.02622\right)q(t)}=-\frac{EI\varphi^{(4)}(x)+P\varphi(x)}{\rho_l\varphi(x)} \quad (31)$$

Let Eq. (31) equal constant , thus

$$\ddot q(t)+\omega^2q(t)+\frac{\eta}{\rho_l}\dot q(t)-\varepsilon\left(Qq^2(t)+Q_1q^3(t)\right)=\varepsilon F_1\cos(\omega_e t+\theta) \quad (32)$$

where

$$F_1=\frac{2.4202\times10^{-3}\cdot K_{q3}II_md}{b\rho_l\bar\varphi\left(d+2w_0+0.01343\right)\left(b+0.02622\right)}\qquad\left(\bar\varphi=\frac{1}{L}\int_0^L\varphi(x)\,dx\right)$$

Letting $\zeta=\varepsilon\zeta_1$, $\omega_e^2=\omega^2(1+\varepsilon\sigma_1)$, $\varphi=\omega_e t$ and

$$\begin{cases}\dfrac{\eta}{\rho_l}=2\zeta\omega\\ Q=\omega^2Q'\\ Q_1=\omega^2Q_1'\\ F_1=\omega^2B_0\end{cases}$$

Substituting Eq. (18) and these equations into Eq. (32), yields

$$\ddot q_0+q_0=0 \quad (33a)$$

$$\ddot q_1+q_1=-\sigma_1\ddot q_0-2\zeta_1\dot q_0+Q'q_0^2+Q'q_0^2+Q_1'q_0^3+B_0(\cos\theta\cos\varphi-\sin\theta\sin\varphi) \quad (33b)$$

……

The solution of zero order equation under above initial conditions is

$$q_0=A\cos\varphi \quad (34)$$

Substituting Eq. (34) into (33(b)), yields

$$\ddot q_1+q_1=\left(\sigma_1A+\frac{3}{4}Q_1'A^3+B_0\cos\theta\right)\cos\varphi+(2\zeta_1A-B_0\sin\theta)\sin\varphi+\frac{Q'A^2}{2}(\cos2\varphi+1)+\frac{Q_1'A^3}{4}\cos3\varphi \quad (35)$$

In order to remove secular item, let

$$\begin{cases}\sigma_1A+\dfrac{3}{4}Q_1'A^3+B_0\cos\theta=0\\ 2\zeta_1A-B_0\sin\theta=0\end{cases} \quad (36)$$

From Eq. (36), we obtain

$$\left[1-\left(\frac{\omega_e}{\omega}\right)^2-\frac{3}{4}Q_1'\varepsilon A^2\right]^2+(2\zeta)^2=\frac{B^2}{A^2} \quad (37)$$

Here $\varepsilon\sigma_1=\left(\omega_e/\omega\right)^2-1$, $\varepsilon\zeta_1=\zeta$ and $\varepsilon B_0=B$.

Letting $\zeta=\zeta\dfrac{\omega_e}{\omega}$ and $\dfrac{\omega_e}{\omega}=s$, yields

$$s^2=1-\frac{3}{4}Q_1'\varepsilon A^2-2\zeta^2\pm\sqrt{\frac{B^2}{A^2}-4\zeta^2\left(1-\frac{3}{4}Q_1'\varepsilon A^2-\zeta^2\right)} \quad (38)$$

6. Results and discussions

Using above equations, the vibration frequencies of the railgun system and their changes along with the system parameters are investigated (see Tables 1-6). For a railgun, the rail and insulator (typically ceramic or polymer

composite) are contained and supported by a containment structure. The containment structure is a steel outer cylinder. The insulator and containment is just the elastic foundation of the rail vibration. The stiffness of the elastic foundation depends on the materials and sizes of the insulator and containment. When the containment material is steel and the insulator material is fiberglass, the stiffness of the elastic foundation is about $4x10^8$ N/m^2-$2x10^{10}$ N/m^2 for containment thickness range 5 mm-40 mm (Tzeng 2003). As smaller stiffness of the elastic foundation is not favorable for the railgun and can cause stronger nonlinearity, stiffness of the elastic foundation is taken as $4x10^8$ N/m^2-$8x10^8$ N/m^2 in this study (see Table 6). Tables 1-6 show:

(1) When the current in the rail grows, the natural frequencies of the railgun system grow because of the effects of the electromagnetic force. The larger is the current, the larger the effects of the electromagnetic force on the natural frequencies. When the current I grows from 0 to 125KA, the natural frequency of the railgun grows from 16770 Hz to 16867 Hz.

As the nonlinearity of the railgun system is considered, the vibration frequencies of the railgun system grow further. When the current in the rail grows, the difference between the natural frequencies and the nonlinear vibration frequencies first becomes large gradually, and then it grows significantly after the current larger than 100KA. For the current of I=125KA, the difference between the natural frequencies and the nonlinear vibration frequencies gets to 42.658%. Here, the nonlinear vibration frequency of the railgun is 29414 Hz which is much larger than the natural frequency of 16770 Hz when the effect of the electromagnetic force is not considered. Therefore, the electromagnetic nonlinearity of the railgun system should be considered when the rail current is relatively large.

(2) When the armature runs on the rail (l grows), the natural frequencies of the railgun system decrease slightly. As the nonlinearity of the railgun system is considered, the vibration frequencies of the railgun system first drop slightly, and then grow significantly with increasing the position l. When the armature runs to 3.5 m, the difference between the natural frequencies and the nonlinear vibration frequencies gets to 10.358%. The results show that the railgun system is a natural frequency changing system caused by the nonlinear electromagnetic force and the force moving on the rail. For large armature position parameter l, the nonlinearity of the railgun system is more obvious and should be considered.

(3) When the distance d between the two rails increases, the natural frequencies of the railgun system drop. As the nonlinearity of the railgun system is considered, the vibration frequencies of the railgun system grow significantly with decreasing the distance d. When the distance d between the two rails is 0.018 m, the difference between the natural frequencies and the nonlinear vibration frequencies gets to 14.470%. The results show that the nonlinearity of the railgun system should be considered for small distance between the two rails.

(4) When the rail thickness b increases, the natural frequencies of the railgun system drop. As the nonlinearity of the railgun system is considered, the vibration frequencies of the railgun system grow. When the rail thickness b drops, the difference between the natural frequencies and the nonlinear vibration frequencies grows. When the rail thickness b is 0.006 m, the difference between the natural frequencies and the nonlinear vibration frequencies gets to 42.865%. It shows that the nonlinearity of the railgun system should be considered for small rail thickness b.

Table 1 Changes of the vibration frequencies along with the current

I(KA)	0	30	50	75	100	125
ω(Hz)	16770	16772	16782	16802	16829	16867
ω_n(Hz)	16770	16856	17226	17440	18747	29414
δ_0(%)	0	0.498	2.573	3.657	10.232	42.658

Here, l=3 m, k=5×10^8 N/m^2, L=5 m, d=0.02 m, h=0.02 m, b=0.01 m

Table 2 Changes of the vibration frequencies with the armature position

$l(m)$	0	1.5	2.5	3	3.5
ω(Hz)	16861	16859	16858	16858	16857
ω_n(Hz)	16861	16859.1	16858.3	18644	18806
δ_0(%)	0	3.77E-07	2.57 E-04	9.575	10.358

Here, I=125KA, k=5×10^8 N/m^2, L=5 m, d=0.02 m, h=0.02 m, b=0.01 m

Table 3 Changes of the vibration frequencies with the distance d

$d(m)$	0.018	0.019	0.02	0.021	0.022	0.023	0.024
ω(Hz)	16867	16861	16856	16851	16846	16842	16838
ω_n(Hz)	19721	18630	18173	17837	17527	17170	16888
δ_0(%)	14.470	9.494	7.246	5.529	3.882	1.907	0.295

Here, I=125KA, k=5×10^8 N/m^2, L=5 m, l=2.5 m, h=0.02 m, b=0.01 m

Table 4 Changes of the vibration frequencies along with the rail thickness b

$b(m)$	0.006	0.007	0.008	0.009	0.010	0.012
ω(Hz)	21781	20162	18857	17776	16861	15388
ω_n(Hz)	38121	21689	19771	18033	17104	15389
δ_0(%)	42.865	7.041	4.625	1.429	1.418	0.00119

Here, I=125KA, k=5×10^8 N/m^2, L=5 m, l=2.5 m, h=0.02 m, d=0.02 m

Table 5 Changes of the vibration frequencies with the rail width *h*

$h(m)$	0.018	0.019	0.02	0.021	0.022	0.023
ω(Hz)	17768	17294	16856	16449	16071	15717
ω_n(Hz)	20602	19010	18173	17484	16840	16154
$\delta_0(\%)$	13.755	9.025	7.246	5.915	4.565	2.702

Here, I=125KA, k=5×10^8 N/m^2, L=5 m, l=2.5 m, b=0.01 m, d=0.02 m

Table 6 Changes of the vibration frequencies along with the stiffness *k*

$k(10^8 N/m^2)$	4	5	6	7	8
ω(Hz)	15093	16852	18444	19909	21273
ω_n(Hz)	16172	17852	19412	20807	22042
$\delta_0(\%)$	6.675	5.605	4.988	4.319	3.491

Here, I=125KA, h=0.02 m, L=5 m, l=2.5 m, b=0.01 m, d=0.02 m

(6) When the stiffness *k* of the elastic foundation increases, the natural frequencies of the railgun system grow. As the nonlinearity of the railgun system is considered, the vibration frequencies of the railgun system grow further. When the stiffness *k* drops, the difference between the natural frequencies and the nonlinear vibration frequencies grows. When the stiffness *k* drops from 8×10^8 N/m^2 to 4×10^8 N/m^2, the difference between the natural frequencies and the nonlinear vibration frequencies grows from 3.491% to 6.675%. It shows that the nonlinearity of the railgun system should be considered for small stiffness *k* of the elastic foundation.

Using Eq. (28), the amplitude-frequency characteristics of the rail system is analyzed (see Figs. 3-7). These figures show:

(1) As the vibrating amplitudes of the rail grow, its vibrating frequencies grow which shows the effects of the electromagnetic nonlinearity on the dynamics performance of the rail system. For a larger current in the rail, the vibrating frequencies of the rail system grow more significantly with the vibrating amplitudes. For small rail distance *d*, the effects of the rail current on the amplitude-frequency characteristics become more obvious. For the same current, the vibrating frequencies of the rail system grow more significantly with the vibrating amplitudes when the rail distance *d* is small.

(2) For small distance *d* between two rails, the vibrating frequencies of the rail system increase more significantly with the vibrating amplitudes of the rail. For the same distance *d*, the vibrating frequencies of the rail system grow more significantly with the vibrating amplitudes when the rail current is large. It shows that the effects of the electromagnetic nonlinearity on the dynamics performance of the rail system are more significant for larger rail current and small distance *d* between two rails.

(3) As the rail thickness *b* or width *h* drops, the vibrating frequencies of the rail system increase more significantly with the vibrating amplitudes of the rail. For small stiffness *k* of the elastic foundation, the vibrating frequencies of the rail system increase more significantly with the vibrating amplitudes of the rail as well. It shows that the effects of the electromagnetic nonlinearity on the dynamics performance of the rail system are more significant for small stiffness *k* of the elastic foundation, small rail thickness *b* or width *h*.

In a word, the electromagnetic nonlinearity has effects on the magnitude-frequency relation of the rail system. The effects of the electromagnetic nonlinearity should be considered for small rail thickness, small rail width, small distance between the two rails, large rail current, and small stiffness *k* of the elastic foundation.

The nonlinear forced responses of the rail to the electromagnetic excitation are investigated. Fig. 8 shows the changes of the nonlinear forced response of the rail with the system parameters.

Fig.8 shows:

(1) As the exciting frequency is near natural frequency of the rail system, the resonance vibration occurs. However, the amplitude-frequency curves bend toward the direction of the exciting frequency increase which shows that at some exciting frequency, the magnitude of vibration will jump from one value to another value. This behavior just is well-known jump phenomenon which corresponds to an unstable operating condition. As the rail current grows, the amplitude-frequency curves bend more obviously toward the direction of the exciting frequency increase, and the frequency range for unstable operating increases obviously.

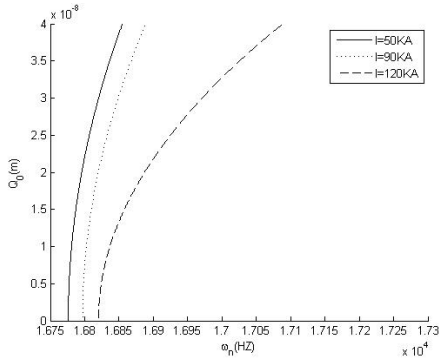

(a) d=30 mm

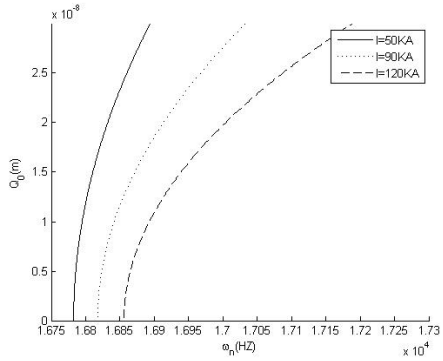

(b) d=20 mm

Fig. 3 Amplitude-frequency characteristics of the rail for various currents)

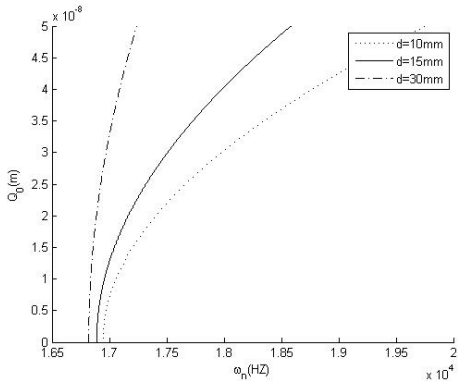

(a) I=120KA

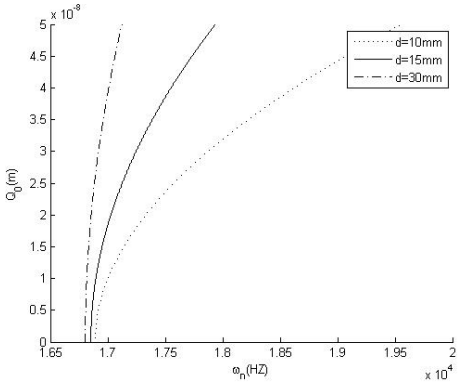

(b) I=100KA

Fig. 4 Amplitude-frequency characteristics of the rail for various *d*

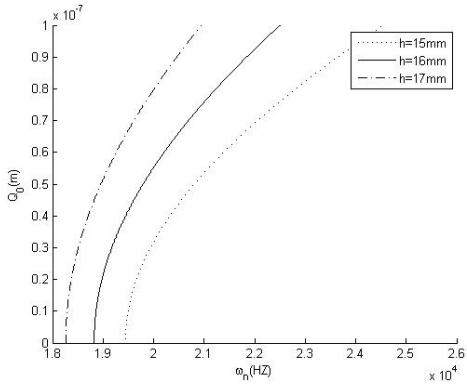

(a) I=105KA

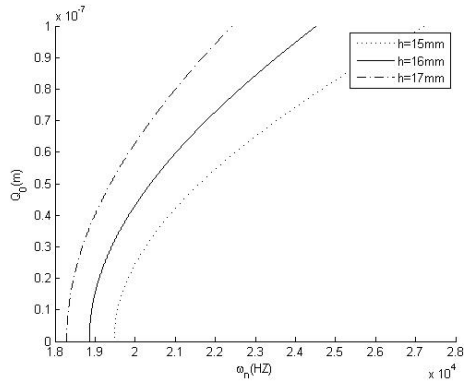

(b) I=125KA

Fig. 6 Amplitude-frequency characteristics of the rail for various rail width *h*

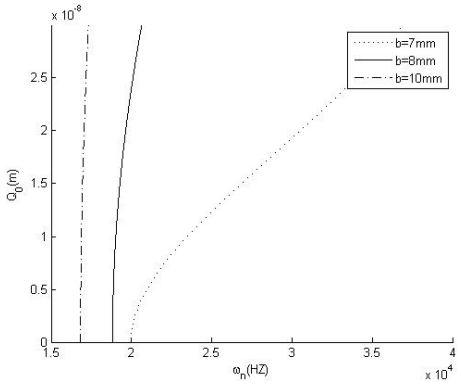

(a) I=100KA

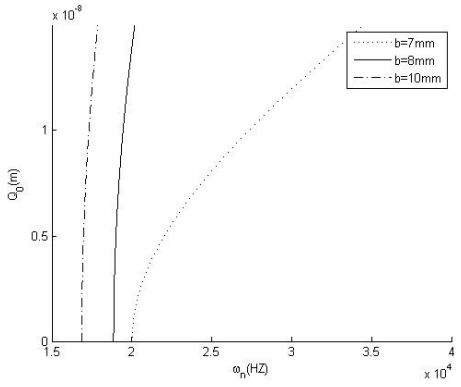

(b) I=125KA

Fig. 5 Amplitude-frequency characteristics of the rail for various rail thickness *b*

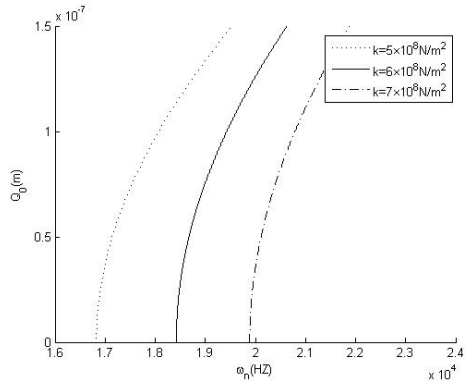

(a) I=100KA

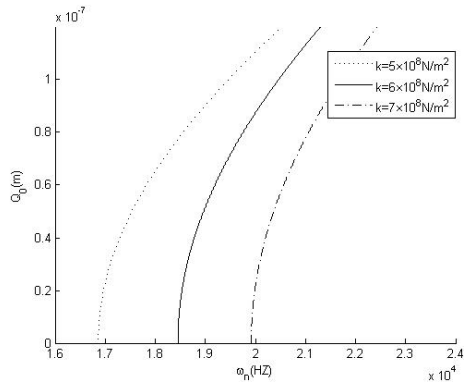

(b) I=125KA

Fig. 7 Amplitude-frequency characteristics of the rail for various stiffness *k*

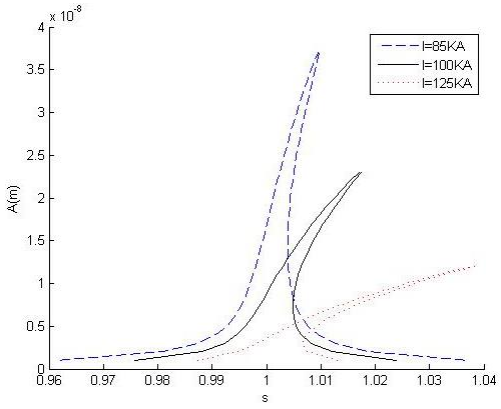

(a) *I* changes

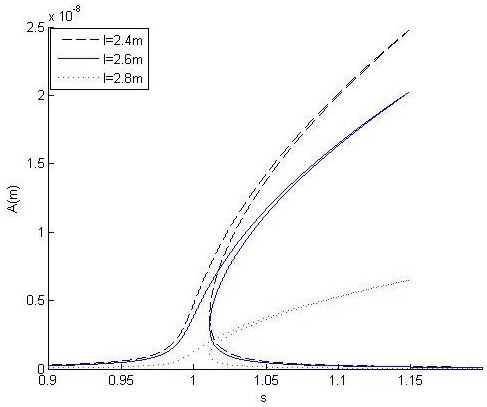

(b) *l* changes

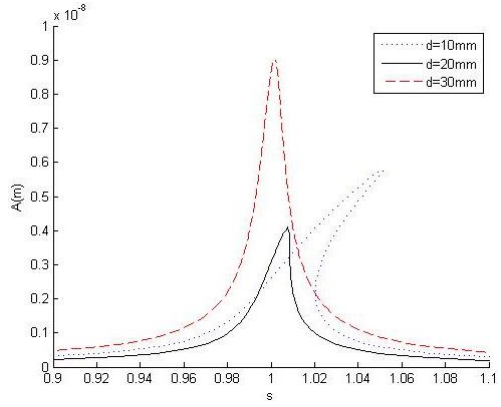

(c) d changes

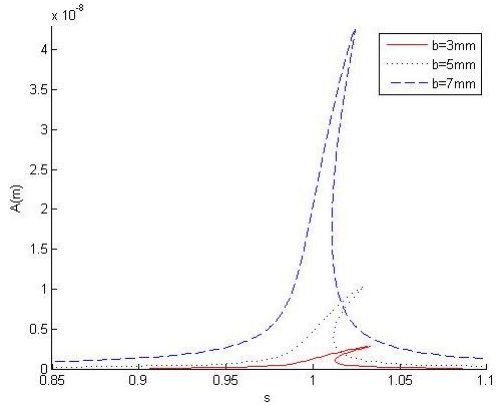

(d) b changes

Continued-

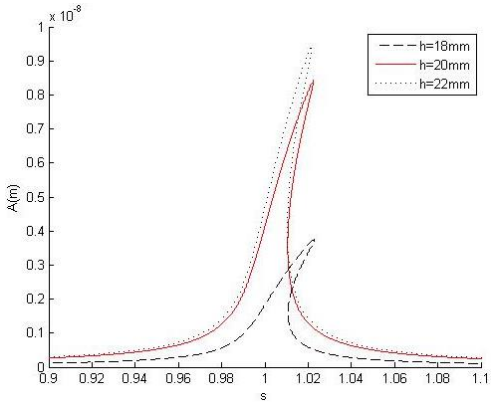

(e) *h* changes

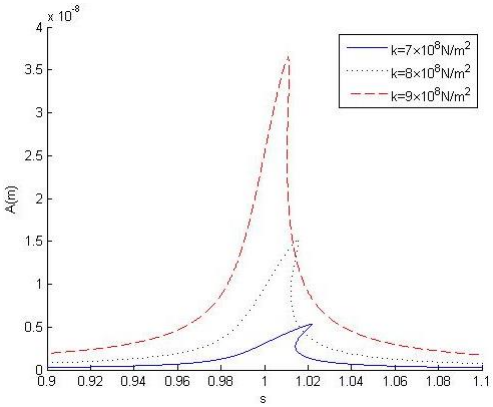

(b) *k* changes

Fig. 8 Nonlinear forced frequency responses of the rail to the electromagnetic excitation

(2) As the rail position coordinate *l* increases, the amplitude-frequency curves bend more obviously toward the direction of the exciting frequency increase, and the frequency range for unstable operation increases obviously. As the distance *d* between two rails drops, the amplitude-frequency curves bend more obviously toward the direction of the exciting frequency increase. As the rail thickness *b* drops, the amplitude-frequency curves bend more obviously toward the direction of the exciting frequency increase as well.

(3) As the rail width *h* drops, the amplitude-frequency curves bend more obviously toward the direction of the exciting frequency increase. As the stiffness *k* of the elastic foundation drops, the amplitude-frequency curves bend more obviously toward the direction of the exciting frequency increase as well. It increases the frequency range for unstable operation obviously.

In a word, the nonlinear electromechanical coupled forced responses of the rail to the electromagnetic excitation are influenced by the rail system parameters. In design of the railgun system, the distance between two rails, the rail current, the rail thickness, the rail width, the rail length, and the stiffness of the elastic foundation should be determined properly to avoid the unstable operating frequency range.

The nonlinear forced time responses of the rail to the electromagnetic excitation are investigated as well (see Fig. 9, here l=1 mm, I_m=50kA). Fig. 9 shows:

(1) When the exciting frequency ω_e is near the first order of the natural frequency ω_1 of the rail gun, the

unstable periodic vibration occurs in the rail. It is because the effects of the multiple frequency components occur.

(2) As the armature runs, after the armature (from 0 to 1 m), the vibrating amplitude of the forced responses of the rail to the electromagnetic load is much larger than that in front of armature (from 1 to 5 m). It means that the undesirable dynamics state of the rail system occurs when the armature runs to the exit. So, the design of the dynamics performance of the rail gun system should be done for this situation.

7. Conclusions

In this paper, the nonlinear electromagnetic force equation of the rail for the railgun is given. In the equation, more system parameters are considered. Based on the equation, the nonlinear electromechanical coupled dynamic equations for the rail are proposed. Using the equations, the nonlinear free vibration frequency of the rail-gun is investigated and the effects of the system parameters on them are analyzed. The nonlinear forced responses of the rail to the electromagnetic excitation are investigated. The results show:

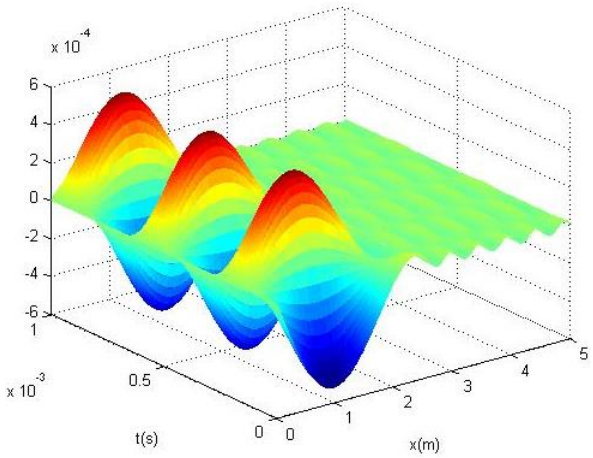

(a) $\omega_e \approx \omega_1 = 16857 rad/s$

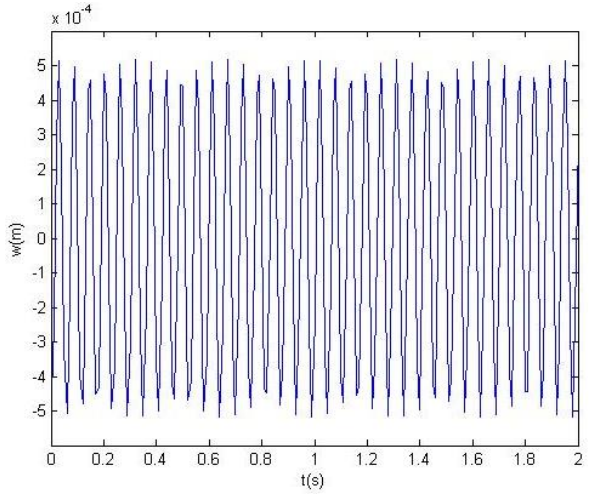

(b) $\omega_e \approx \omega_1$, $x=l$

Fig. 9 Amplitude-frequency characteristics of the rail for various *d*

(1) As the nonlinearity of the railgun system is considered, the vibration frequencies of the railgun system increase. As the current in the rail grows, the difference between the natural frequencies and the nonlinear vibration frequencies grows significantly. So, the nonlinearity of the railgun system should be considered when the rail current is relatively large.

(2) The railgun system is a natural frequency changing system caused by the nonlinear electromagnetic force and the armature moving on the rail. For large armature position, the nonlinearity of the railgun system is more significant. The nonlinearity of the railgun system is more obvious for small distance between the two rails, small rail thickness, and small stiffness of the elastic foundation.

(3) As the rail current or the rail position coordinate grows, the unstable frequency range increases obviously. As the distance between two rails, the rail thickness, the rail width or the stiffness of the elastic foundation drop, the unstable frequency range increases obviously as well. In design of the railgun system, the rail current or the rail length should be taken as small values, and the distance between two rails, the rail thickness, rail width or the stiffness of the elastic foundation should be taken as large values.

(4) When the armature runs to the exit, the vibrating amplitude of the forced responses of the rail to the electromagnetic load is largest. So, the design of the dynamics performance of the rail gun system should be done for this situation.

Acknowledgements

This project is supported by the Doctoral Research Program Foundation of Education Ministry of China (Priority development areas, no. 20131333130002).

References

Fair, H. (2007), "Progress in electromagnetic launch science and technology", *IEEE T. Magnetics*, **43**(1), 93-98.

Fryba, L. (1977), *Vibration of Solids and Structures under Moving Loads*, Gronningen, The Netherlands: Noordhoff.

Geng, Y. (2013), "Electromechanical coupled dynamics of rails for electromagnetic launcher", *Int. J. Appl. Electrom. Mech.*, **42**(3), 369-389.

He, W. and Bai, X. (2013), "Dynamic responses of rails and panels of rectangular electromagnetic rail launcher", *J. Vib. Shock*, **32**(15), 144-148 (in China).

Johnson, A. and Moon, F. (2006), "Elastic waves and solid armature contact pressure in electromagnetic launchers", *IEEE T. Magnetics*, **42**(3), 422-429.

Johnson, A. and Moon, F. (2007), "Elastic waves in electromagnetic launchers", *IEEE T. Magnetics*, **43**(1), 141-144.

Lehmann, P., Peter, H. and Wey, J. (2001), "First experimental results with the ISL 10-MJ-DES railgun PEGASUS", *IEEE T. Magnetics*, **37**(1), 435-439.

Nechitailo, N. and Lewis, B. (2006), "Critical velocity for rails in hypervelocity launchers", *Int. J. Impact Eng.*, **33**(1-12), 485-495.

Pai, P.F. and Kaufman, C.A. (2012), "Characteristic speeds and influences of cross-sectional warpings on high-speed beam-foundation structures", *Int. J. Mech. Sci.*, **59**(1), 8-21.

Schuppler, C., Tumonis, L., Kačianauskas, R. and Schneider, M. (2013), "Experimental and numerical investigations of vibrations at a railgun with discrete supports", *IEEE T. Plasma Sci.*, **41**(5),

1508-1513.
Shvetsov, G., Rutberg, P. and Budin, A. (2007), "Overview of some recent EML research in Russia", *IEEE T. Magnetics*, **43**(1), 99-106.
Tumonis, L., Schneider, M., Kaèianauskas, R. and Kaèeniauskas, A. (2009), "Structural mechanics of railguns in the case of discrete supports," *IEEE T. Magnetics*, **45**(1), 474-479.
Tzeng, J. (2003), "Dynamic response of electromagnetic railgun due to projectile movement", *IEEE T. Magnetics*, **39**(1), 472-475.
Tzeng, J. and Sun, W. (2007), "Dynamic responce of cantilevered rail guns attributed to projectile/gun interaction - theory". *IEEE T. Magnetics*, **43**(1), 207-213.
Xu, L. and Geng, Y. (2012), "Dynamics of rails for electromagnetic railguns", *Int. J. Appl. Electrom.Mech.*, **38**(1), 47-64.
Xu, L., Zheng, F. and Peng, L. (2015), "Electromechanical coupled nonlinear free vibration of rails for electromagnetic railguns", *Int. J. Appl. Electrom. Mech.*, **47**(2), 313-322.

CC

Appendix. Solutions of the linear natural frequencies for the railgun system

The mode function is considered as

$$\phi(\theta) = e^{\lambda\theta} \tag{A1}$$

Substituting (A1) into (16), then

$$\lambda^4 - R = 0 \tag{A2}$$

At $R > 0$ ($\omega^2 \rho_l > P$), the solutions of Eq. (A2) are $\pm\sqrt[4]{R}$ and $\pm i\sqrt[4]{R}$. Then, the general solution of Eq. (16) is

$$\phi_1(x) = A_1 e^{mx} + A_2 e^{-mx} + A_3 \cos mx + A_4 \sin mx \tag{A3}$$

where $m = \sqrt[4]{R}$

When $R < 0$ ($\omega^2 \rho_l < P$), the solutions of Eq. (A2) are $\frac{\sqrt{2}}{2}\sqrt[4]{-R} \pm i\frac{\sqrt{2}}{2}\sqrt[4]{-R}$ and $-\frac{\sqrt{2}}{2}\sqrt[4]{-R} \pm i\frac{\sqrt{2}}{2}\sqrt[4]{-R}$. Then, the general solution of Eq. (16) is

$$\phi_1(x) = e^{n_1 x}\left(A_1 \cos n_1 x + A_2 \sin n_1 x\right) + e^{n_2 x}\left(A_3 \cos n_2 x + A_4 \sin n_2 x\right) \tag{A4}$$

where $n_1 = \frac{\sqrt{2}}{2}\sqrt[4]{-R}$ and $n_2 = -\frac{\sqrt{2}}{2}\sqrt[4]{-R}$

Substituting $\phi(\theta) = e^{\lambda\theta}$ into (17), then

$$\lambda^4 - S^4 = 0 \tag{A5}$$

The solutions of Eq. (A5) are $\pm S$ and $\pm iS$. Then, the general solution of Eq. (17) is

$$\phi_2(x) = A_5 e^{Sx} + A_6 e^{-Sx} + A_7 \cos Sx + A_8 \sin Sx \tag{A6}$$

The constants $A_j\,(j = 1,2,3,4,5,6,7,8)$ are obtained by boundary conditions and the continuity conditions of the rail.

For the simply supported rail at two ends, the boundary conditions are

$$\begin{cases} \phi_1(0) = 0 \\ \phi_2(L) = 0 \\ \phi_1''(x)\big|_{x=0} = 0 \\ \phi_2''(x)\big|_{x=L} = 0 \end{cases} \tag{A7}$$

The continuity conditions of the rail are

$$\begin{cases} \phi_1(l) = \phi_2(l) \\ \phi_1'(l) = \phi_2'(l) \\ \phi_1''(l) = \phi_2''(l) \\ \phi_1'''(l) = \phi_2'''(l) \end{cases} \tag{A8}$$

At $R > 0$, substituting Eqs. (A3) and (A6) into (A7) and (A8), yields $A_3 = 0$ and

$$C_1 X_1 = D_1 \tag{A9}$$

where

$$C_1 = \begin{bmatrix} 1 & 1 & 0 & 0 & 0 & 0 & 0 \\ 0 & 0 & 0 & e^{SL} & e^{-SL} & \cos SL & \sin SL \\ 0 & 0 & 0 & S^2 e^{SL} & S^2 e^{-SL} & -S^2 \cos SL & -S^2 \sin SL \\ e^{ml} & e^{-ml} & \sin ml & -e^{Sl} & -e^{-Sl} & -\cos Sl & -\sin Sl \\ me^{ml} & -me^{-ml} & m\cos ml & -Se^{Sl} & Se^{-Sl} & S\sin Sl & -S\cos Sl \\ m^2 e^{ml} & m^2 e^{-ml} & -m^2 \sin ml & -S^2 e^{Sl} & -S^2 e^{-Sl} & S^2 \cos Sl & S^2 \sin Sl \\ m^3 e^{ml} & -m^3 e^{-ml} & -m^3 \cos ml & -S^3 e^{Sl} & S^3 e^{-Sl} & -S^3 \sin Sl & S^3 \cos Sl \end{bmatrix}$$

$$X_1 = \begin{bmatrix} A_1 & A_2 & A_4 & A_5 & A_6 & A_7 & A_8 \end{bmatrix}^T$$

$$D_1 = \begin{bmatrix} 0 & 0 & 0 & 0 & 0 & 0 & 0 \end{bmatrix}^T$$

The condition that non zero coefficients $A_j\,(j = 1,2,4,5,6,7,8)$ exist is

$$\begin{vmatrix} 1 & 1 & 0 & 0 & 0 & 0 & 0 \\ 0 & 0 & 0 & e^{SL} & e^{-SL} & \cos SL & \sin SL \\ 0 & 0 & 0 & S^2 e^{SL} & S^2 e^{-SL} & -S^2 \cos SL & -S^2 \sin SL \\ e^{ml} & e^{-ml} & \sin ml & -e^{Sl} & -e^{-Sl} & -\cos Sl & -\sin Sl \\ me^{ml} & -me^{-ml} & m\cos ml & -Se^{Sl} & Se^{-Sl} & S\sin Sl & -S\cos Sl \\ m^2 e^{ml} & m^2 e^{-ml} & -m^2 \sin ml & -S^2 e^{Sl} & -S^2 e^{-Sl} & S^2 \cos Sl & S^2 \sin Sl \\ m^3 e^{ml} & -m^3 e^{-ml} & -m^3 \cos ml & -S^3 e^{Sl} & S^3 e^{-Sl} & -S^3 \sin Sl & S^3 \cos Sl \end{vmatrix} = 0 \tag{A10}$$

At $R < 0$, substituting Eqs. (A4) and (A6) into (A7) and (A8), yields

$$C_2 X_2 = D_2 \tag{A11}$$

where

$$C_2 = \begin{bmatrix} 1 & 0 & 1 \\ 0 & 0 & 0 \\ 0 & n_1^2 & 0 \\ 0 & 0 & 0 \\ e^{n_1 l}\cos n_1 l & e^{n_1 l}\sin n_1 l & e^{n_2 l}\cos n_2 l \\ n_1 e^{n_1 l}(\cos n_1 l - \sin n_1 l) & n_1 e^{n_1 l}(\cos n_1 l + \sin n_1 l) & n_2 e^{n_2 l}(\cos n_2 l - \sin n_2 l) \\ -2n_1^2 e^{n_1 l}\sin n_1 l & 2n_1^2 e^{n_1 l}\cos n_1 l & -2n_2^2 e^{n_2 l}\sin n_2 l \\ -2n_1^3 e^{n_1 l}(\cos n_1 l + \sin n_1 l) & 2n_1^3 e^{n_1 l}(\cos n_1 l - \sin n_1 l) & -2n_2^3 e^{n_2 l}(\cos n_2 l + \sin n_2 l) \end{bmatrix}$$

$$\begin{bmatrix} 0 & 0 & 0 & 0 & 0 \\ 0 & e^{SL} & e^{-SL} & \cos SL & \sin SL \\ n_2^2 & 0 & 0 & 0 & 0 \\ 0 & S^2 e^{SL} & S^2 e^{-SL} & -S^2 \cos SL & -S^2 \sin SL \\ e^{n_2 l}\sin n_2 l & -e^{Sl} & -e^{-Sl} & -\cos Sl & -\sin Sl \\ n_2 e^{n_2 l}(\cos n_2 l + \sin n_2 l) & -Se^{Sl} & Se^{-Sl} & S\sin Sl & -S\cos Sl \\ 2n_2^2 e^{n_2 l}\cos n_2 l & -S^2 e^{Sl} & -S^2 e^{-Sl} & S^2 \cos Sl & S^2 \sin Sl \\ 2n_2^3 e^{n_2 l}(\cos n_2 l - \sin n_2 l) & -S^3 e^{Sl} & S^3 e^{-Sl} & -S^3 \sin Sl & S^3 \cos Sl \end{bmatrix}$$

$$X_2 = \begin{bmatrix} A_1 & A_2 & A_3 & A_4 & A_5 & A_6 & A_7 & A_8 \end{bmatrix}^T$$

$$D_2 = \begin{bmatrix} 0 & 0 & 0 & 0 & 0 & 0 & 0 & 0 \end{bmatrix}^T$$

The condition that non zero coefficients $A_j\,(j = 1,2,3,4,5,6,7,8)$ exist is

$$\begin{vmatrix} 1 & 0 & 1 \\ 0 & 0 & 0 \\ 0 & n_1^2 & 0 \\ 0 & 0 & 0 \\ e^{n_1 l}\cos n_1 l & e^{n_1 l}\sin n_1 l & e^{n_2 l}\cos n_2 l \\ n_1 e^{n_1 l}(\cos n_1 l - \sin n_1 l) & n_1 e^{n_1 l}(\cos n_1 l + \sin n_1 l) & n_2 e^{n_2 l}(\cos n_2 l - \sin n_2 l) \\ -2n_1^2 e^{n_1 l}\sin n_1 l & 2n_1^2 e^{n_1 l}\cos n_1 l & -2n_2^2 e^{n_2 l}\sin n_2 l \\ -2n_1^3 e^{n_1 l}(\cos n_1 l + \sin n_1 l) & 2n_1^3 e^{n_1 l}(\cos n_1 l - \sin n_1 l) & -2n_2^3 e^{n_2 l}(\cos n_2 l + \sin n_2 l) \end{vmatrix}$$

$$\begin{vmatrix} 0 & 0 & 0 & 0 & 0 \\ 0 & e^{SL} & e^{-SL} & \cos SL & \sin SL \\ n_2^2 & 0 & 0 & 0 & 0 \\ 0 & S^2 e^{SL} & S^2 e^{-SL} & -S^2 \cos SL & -S^2 \sin SL \\ e^{n_2 l}\sin n_2 l & -e^{Sl} & -e^{-Sl} & -\cos Sl & -\sin Sl \\ n_2 e^{n_2 l}(\cos n_2 l + \sin n_2 l) & -Se^{Sl} & Se^{-Sl} & S\sin Sl & -S\cos Sl \\ 2n_2^2 e^{n_2 l}\cos n_2 l & -S^2 e^{Sl} & -S^2 e^{-Sl} & S^2 \cos Sl & S^2 \sin Sl \\ 2n_2^3 e^{n_2 l}(\cos n_2 l - \sin n_2 l) & -S^3 e^{Sl} & S^3 e^{-Sl} & -S^3 \sin Sl & S^3 \cos Sl \end{vmatrix} = 0 \tag{A12}$$

Eq. (A12) can give linear natural frequencies of the railgun system.